The Manipulation of Photon Spatial Wave Function by Polarization and Parity

Deepika Sundarraman
Physics Department, The College of Wooster, Wooster, Ohio 44691, USA
(Dated: May 9, 2013)

We investigate interference of light in classical optics based on a one-dimensional parity transformation. The manipulation of the photon spatial wave function is used to predict Hong Ou Mandel interference (HOMI), which has applications to quantum information processing. This effect is achieved by manipulating two degrees of freedom, namely, the parity and polarization of the photon spatial wave function. Plots for the interferometer outputs in the case of classical interference are studied in the form of density plots of intensity distributions, and plots of polarization ellipses. Inferences are drawn to predict the relationship between these two degrees of freedom and whether they are relevant to HOMI and quantum computing. Theoretical predictions are made for both single and two input case, the latter of which can then be extrapolated to HOMI. HOMI is predicted to occur for any case where completely destructive interference is present in one output port in the corresponding classical situation. A special case to keep both degrees of freedom independent of each other during transmission was found, when two identical inputs of HG_{01} modes with $\hat{x}+\hat{y}$ polarization are introduced in the interferometer. Further, another means to mix polarization and parity are found when two HG_{+45} spatial modes with $\hat{x}+\hat{y}$ polarization are introduced as inputs. These cases have been modeled using a simulation in Mathematica. The results from various predictions for classical beams thus help us gather intuition for the behavior of photons.

I. INTRODUCTION

One of the phenomena of linear optics useful for quantum computing is Hong Ou Mandel Interference. Hong, Ou and Mandel proposed a theory [1] in 1987 that involves two photon interference in a beam splitter resulting in both photons exiting out of the same output port of the beam splitter due to quantum indistinguishability. This is shown conceptually in Fig.1. Here the quantum probability of two photons being reflected and two photons being transmitted cancel by phase difference. This outcome is a result of quantum indistinguishability.

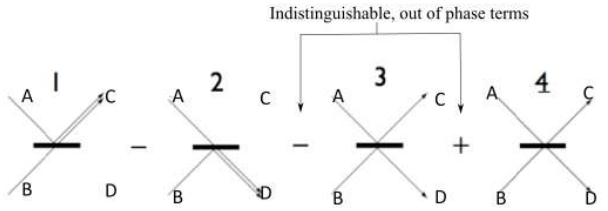

FIG. 1: A schematic of Hong Ou Mandel Interference using a beamsplitter: The quantum probabilities of both photons reflecting and both transmitting cancel by virtue of phase

Quantum indistinguishability is the property by virtue of which the output photons from the interferometer are in the same quantum state and hence indistinguishable. The output states of the two photons, when both exit out of the same port of the beam splitter, are entangled by the principle of quantum mechanics which means that the state of one photon is directly correlated to the state of the other photon. This theory is the basis for quantum computing. This theory can be exploited in more complex optical systems involving interferometers. The theoretical models of classical situations such as laser beams instead of photons are studied to gain intuition on the behavior of photons and extend the case to two photon interference in quantum optics.

The beginning of the project involves introducing classical light described by an arbitrary spatial mode into a single input of a one dimensional interferometer, where the outputs get sort out into the fundamental spatial modes. This kind of device is called a one dimensional sorter. This is then expanded to include two inputs and HOMI of the outputs is the investigated as done in previous research [2] and [3] on the same experiment. The new difference from previous experiments and theoretical predictions is that now we are able to manipulate another degree of freedom of the input beam, polarization.

The ability to control two degrees of freedom, that is the manipulation of the photon spatial wave function in terms of polarization and parity can allow for us the capability in quantum information processing to send two bits of information that do not interact with each other and can be transported concurrently but independent of the other.

At the same time a means to cause interactions among the two degrees of freedom might allow one to create entangled states, such that, we can determine polarization information about one photon when we know spatial mode information of the other. This can also be used for quantum computing.

The applications of this work span across various disciplines. In molecular biology these spatial modes and interferometers discussed in this paper can be used for the variable control over the spatial mode profile of optical tweezers, which have been used to impart orbital angular momentum to microscopic particles, and probe the mechanics of RNA transcription.[4]. The investigated two photon entangled states can be used for enhanced resolution of light-sensitive microscopic objects via quantum imaging techniques.

FIG. 2: A density plot describing the HG_{00} zeroth order mode

FIG. 3: A density plot describing the HG_{01}, first order Hermite Gaussian 'even' mode

FIG. 4: A density plot describing the HG_{10}, first order Hermite Gaussian 'odd' mode

II. THEORY

A. Even-Odd Polarized Modes

Light can be described in the form of Hermite Gaussian modes. The electric field due to a Hermite Gaussian mode [5] in the x-y plane is given by,

$$E(x,y,0) \equiv \mid HG_{nm}\rangle = \frac{A_{nm}}{w_0} H_n(\frac{\sqrt{2}x}{w_0}) H_m(\frac{\sqrt{2}y}{w_0}) e^{-(x^2+y^2)} \tag{1}$$

where A_{nm} is the normalization constant, w_0 is the beam width and H_n and H_m are Hermite polynomials that can be computed for positive integer values of n and m respectively. x and y are the electric fields in the x and the y directions of the mode respectively. These Hermite Gaussian modes are visualized in terms of their intensity distribution [3] which can be found from the electric field as

$$I = |E(x,y,0)|^2 = |HG_{nm}|^2. \tag{2}$$

The HG_{00} mode or the zeroth order mode in Fig. 2 is commonly referred to as the Gaussian mode and can be simply understood as the light emitted from standard laser cavities. The other spatial modes that are useful for this project are the first order modes HG_{01} and HG_{10} which are shown in Fig. 3 and Fig. 4. These modes can be simplified from the above Eq. 1 as,

$$HG_{01} = \frac{1}{\pi} H_0(\sqrt{2}x) H_1(\sqrt{2}y) e^{-(x^2+y^2)} \tag{3}$$

$$HG_{10} = \frac{1}{\pi} H_1(\sqrt{2}x) H_0(\sqrt{2}y) e^{-(x^2+y^2)}. \tag{4}$$

These even and odd modes are then used to build our fundamental basis for our quantum computational Bloch sphere that represents all the possible superpositions of these two fundamental modes. Each mode on the Bloch sphere can be described by the coordinates θ and ϕ in spherical coordinates. Thus any point on the Bloch sphere in this coordinate system is given by $(\sin\theta\cos\phi, \sin\theta\sin\phi, \cos\theta)$. Some of the modes which were relevant to our project are shown in Fig. 5.

Thus, we draw up a means to mathematically represent arbitrary spatial modes for our project. Here, we consider a general optical system comprising two input ports A and B each of which has a certain two dimensional photonic state of the spatial mode given by

$$[\cos\theta \mid HG_{01}\rangle x + e^{i\phi}\sin\theta \mid HG_{10}\rangle][\cos\beta\hat{y} + e^{i\alpha}\sin\beta\vec{x}] \tag{5}$$

where the state $|HG_{01}\rangle$ is the even Hermite Gaussian mode described pictorially in Fig. 3 and the $|HG_{10}\rangle$ is the odd Hermite Gaussian mode shown in Fig. 4 and $\hat{y}$ is a vertical polarization i.e. polarization in the y-direction whereas $\hat{x}$ is horizontal polarization in the x-direction. The coefficients $\cos\theta$, $e^{i\phi}\sin\theta$, $\cos\beta$ and $e^{i\alpha}\sin\beta$ determine the magnitude of electric field in each degree of freedom. Here, θ and ϕ are the spherical coordinates on the Bloch sphere, whereas α and β are the spherical coordinates that describe polarization on the Poincare sphere. The simplification of Eq. 5 above gives rise to four terms in the form of,

$$\cos\theta\cos\beta\vec{E}_{00} + e^{i(\phi+\alpha)}\sin\theta\sin\beta\vec{E}_{11} + e^{i\alpha}\cos\theta\sin\beta\vec{E}_{01} + e^{i\phi}\sin\theta\cos\beta\vec{E}_{10}. \tag{6}$$

The new states represent a combination of parity and polarization such that $\vec{E_{00}}$ is the even spatial mode y-direction polarized state, the electric field [6] of which can be visualized in Fig. 6. The red and blue colors on the lobes of the electric field in Fig. 6 describe the sign of the electric field in space, where red stands for negative and blue for positive electric field. Note that these are different from the intensity distributions that are always positive and hence blue. Similarly, $\vec{E}_{11}$ that is shown in Fig. 7 is the odd spatial mode, x-direction polarized

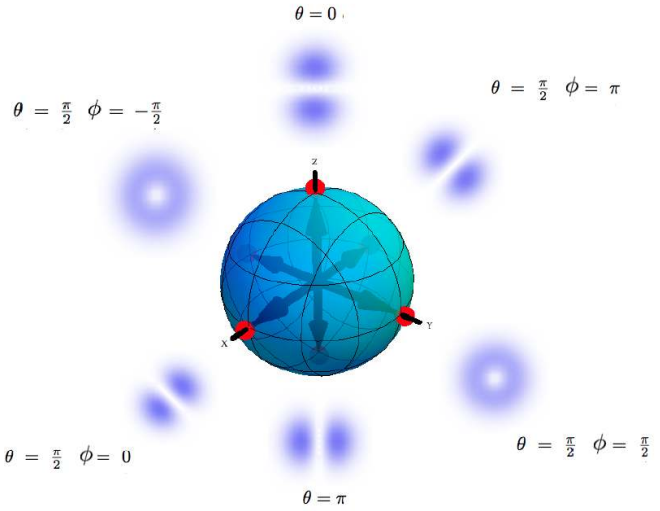

FIG. 5: A schematic of the quantum computational Bloch sphere with all fundamental spatial modes. The polar angle is represented by θ and ϕ is the azhimuthal angle.

state whereas $\vec{E}_{01}$ in Fig. 8, is the even spatial mode, x-direction polarized state. Lastly, $\vec{E}_{10}$ is the odd spatial mode y-direction polarized state represented in Fig. 9.

Thus, our fundamental equation with polarization and parity has been transformed into four basis states which we will commonly refer to as 'modes' to be visualized in Fig. 5. The notation we use for this project i.e. $\vec{E}_{nm}$ where n and m can be 0 or 1, must be noted to realize that when we add the subscripts of these modes, we get 'net odd' and 'net even' combinations of modes that tell you what happens to these modes when they interact with mirrors, incurring parity flips. Thus, when a $\vec{E}_{00}$ mode interacts with a mirror, we find that (0+0=even), thus no net flip in mode, whereas, $\vec{E}_{01}$ (0+1=odd) encounters a net flip that can be visualized in Fig. 10

The system that we want to create to be able to manipulate two degrees of freedom, namely, parity and polarization, can be separately understood in the form of two spheres. These spheres are tools to understand an orthogonal basis that comprises two mutually independent states. A spatial mode sphere, commonly called a Bloch sphere shows an orthogonal system of the odd spatial mode shown in Fig. 3 and the even spatial mode represented in Fig. 4. Similarly, polarization also has this kind of an orthogonal basis with vertical and horizontal polarization being on two poles of such a sphere [7], which is commonly referred to as a Poincare sphere in the field of optics. This Bloch sphere representation can be conveniently used to describe our modes as can be seen in Fig. 5 , in such a manner that every point on the sphere is a representation of a mode with a certain value of θ and ϕ, thus being superpositions of the orthogonal even-odd basis.

Similarly, every point on the Poincare sphere is a unique representation of a polarization state, that is superposition of the vertical and horizontal polarizations having specific values of β and α. Through our theoretical analysis, the combination of the two spheres would be needed to create a four-dimensional basis that takes into account four fundamental bases, $\vec{E_{00}}$, $\vec{E_{11}}$, $\vec{E_{01}}$ and $\vec{E_{10}}$. Some of the interesting modes and polarizations we investigate, are shown on the equator of these two spheres as can be visualized for the Bloch sphere in Fig. 5 and

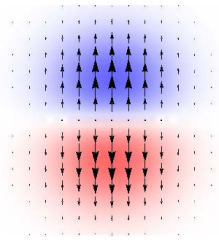

FIG. 6: A vector field plot of the $\vec{E}_{00}$ state i.e. even y-polarized mode

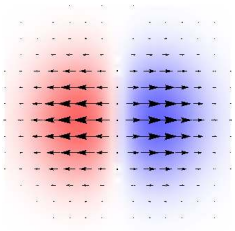

FIG. 7: A vector field plot of the $\vec{E}_{11}$ state, i.e. odd x-polarized mode

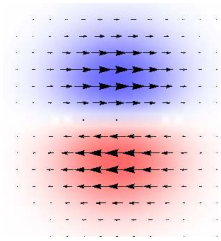

FIG. 8: A vector field plot of the $\vec{E}_{01}$ state, i.e. even x-polarized mode

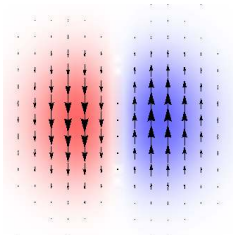

FIG. 9: A vector field plot of the $\vec{E}_{10}$ state, i.e. odd x-polarized mode

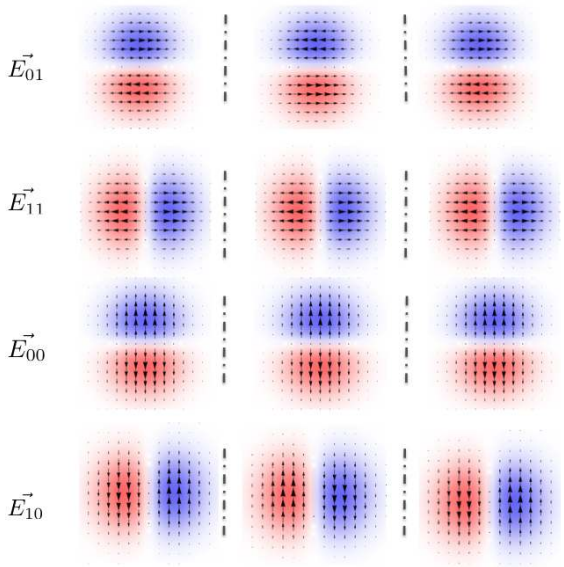

FIG. 10: A schematic of the mirror flips associated with the various modes. The first column represents the fundamental mode while the second and third column represent mirror flips(a reflection on the mirror) on these modes in the $\hat{x}$ direction.

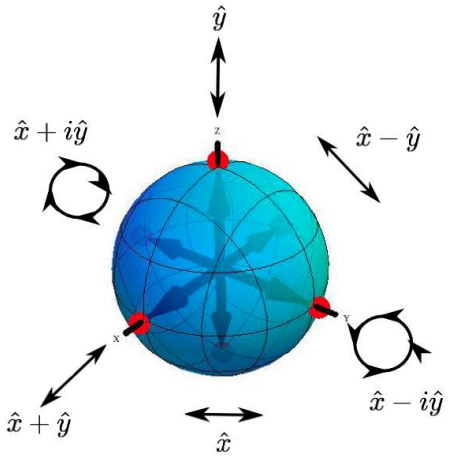

FIG. 11: A representation of the Polarization Sphere with vertical and horizontal polarization on the poles.The superposition of these creates 45° linear and circular polarizations shown on the equator of the sphere.

for the Poincare sphere in Fig. 12.

B. Interferometry

For the purpose of achieving Hong Ou Mandel interference, Hong, Ou and Mandel used a beam splitter as illustrated in Fig. 1. In our experiment, we use a Mach Zehnder interferometer with some extra components. Firstly, there is an extra mirror on one arm. Second, we create a phase difference between the two arms with a glass plate

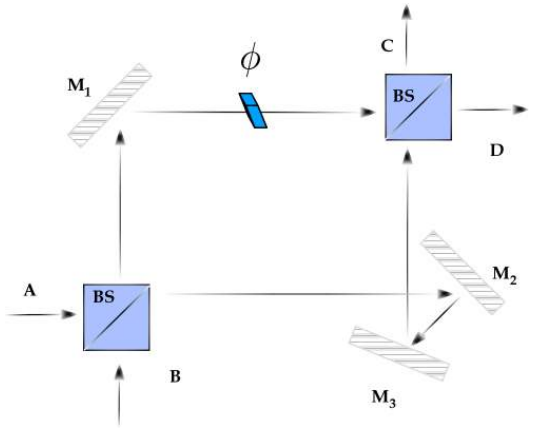

FIG. 12: The Mach Zehnder Interferometer with an extra mirror on one arm and an extra glass plate in the other

only on one arm that causes a lag in path length of the beam by Snell's law. The elements of this engineered interferometer give us the ability to be able to manipulate the arbitrary spatial modes and the means by which they interact with various elements of the interferometer in Fig. 6. The key technique used to analyze these interactions are matrices used in linear optics. The matrix methods used in optics follow simple linear algebra rules and can take into account multiple optical interfaces by the simple multiplication of various elements in sequence (right to left) such that we arrive at one 'master' matrix that multiplies the inputs to give the outputs of the interferometer. The inputs A and B, and outputs C and D can thus be related as

$$\begin{pmatrix} e_{00}^{c} \\ e_{00}^{d} \\ e_{10}^{c} \\ e_{10}^{d} \\ e_{11}^{c} \\ e_{11}^{d} \\ e_{01}^{c} \\ e_{01}^{d} \end{pmatrix} = \widehat{U}_{(8\times 8)} \begin{pmatrix} e_{00}^{a} \\ e_{00}^{b} \\ e_{10}^{a} \\ e_{10}^{b} \\ e_{11}^{a} \\ e_{11}^{b} \\ e_{01}^{a} \\ e_{01}^{b} \end{pmatrix}, \tag{7}$$

where e_{00}^{c} represents the output of port 'C' with $\mid 00\rangle$ state i.e. even mode with vertical polarization. Similarly, e_{10}^{a} represents the input, in port 'A' with $\mid 10\rangle$ state, i.e. odd mode with vertical polarization and so on. The $\widehat{U}_{(8\times 8)}$ represents the 'master' matrix with all the elements in the interferometer multiplied out to leave us with one matrix. This matrix has a special property of being unitary, which means.

$$\widehat{U}.\widehat{U}^{*} = I \tag{8}$$

where $\widehat{U}^{*}$ is the transpose conjugate of the $\widehat{U}$ matrix and I is the identity matrix.

TABLE I: A table showing the Matrix representations of the various elements of the interferometer [2] and [3].

Optical Element	$\widehat{U}$ representation	Matrix
Beam Splitter	$\widehat{U}_{BS}$	$\begin{pmatrix} 1 & i\Pi \\ i\Pi & 1 \end{pmatrix}$
Mirror	$\widehat{U}_{M}$	$\begin{pmatrix} 1 & 0 \\ 0 & \Pi \end{pmatrix}$
Glass Plate	$\widehat{U}_{GP}$	$e^{i\frac{\delta}{2}}\begin{pmatrix} e^{i\frac{\delta}{2}} & 0 \\ 0 & e^{-i\frac{\delta}{2}} \end{pmatrix}$

C. $\widehat{U}$ Matrix

The $\widehat{U}$ matrix is used to describe the interferometer elements that interact with the inputs to give the outputs. From Table I we can find the various matrix representations of each optical element. For an arbitrary input from port A, say E^a_{ij} and and an arbitrary input from port B, say E^b_{ij} we have a certain output E^c_{ij}, out of port C and E^d_{ij} out of port D. Here, i and j can be either 0 or 1, to give the various fundamental mode. Thus we are trying to find the arbitrary outputs of the fundamental mode, E_{ij} out port C and D when, E_{ij} is introduced into the interferometer from inputs A and B.

$$\begin{pmatrix} E^c_{ij} \\ E^d_{ij} \end{pmatrix} = \widehat{U}_{(2\times 2)} \begin{pmatrix} E^a_{ij} \\ E^b_{ij} \end{pmatrix}. \tag{9}$$

Note that the $\widehat{U}_{2\times 2}$ is a condensed form of of the earlier $\widehat{U}$ that was 8×8 in dimension from Eq. 7. The new 2×2 makes it algebraically simpler to tackle a number of matrix computations for all the odd(i.e. 01,10) and even modes(ie. 00,11) at once as the outcomes for all the even spatial modes are the same on encountering mirrors i.e. they don't encounter flips. Similarly, the odd spatial modes would undergo flips on mirrors. Thus, this notation is powerful in evaluating the outputs for arbitrary even or odd inputs in A and B ports to give us the outputs from C and D ports. From the sequence of events on the inputs, going from right to left we determine,

$$\widehat{U} = \widehat{U}_{BS}\widehat{U}_{M}\widehat{U}_{GP}\widehat{U}_{BS}. \tag{10}$$

Corresponding to Table I we have,

$$\widehat{U} = \frac{1}{2}e^{i\frac{\delta}{2}} \begin{pmatrix} 1 & i\Pi \\ i\Pi & 1 \end{pmatrix} \begin{pmatrix} e^{i\frac{\delta}{2}} & 0 \\ 0 & e^{-i\frac{\delta}{2}} \end{pmatrix} \begin{pmatrix} 1 & 0 \\ 0 & \Pi \end{pmatrix} \begin{pmatrix} 1 & i\Pi \\ i\Pi & 1 \end{pmatrix} \tag{11}$$

where Π is the parity operator associated with reflections due to the beam splitter and the mirror [8]. This can take a value of +1 when the original spatial mode is retained after the reflection or -1 when the spatial mode flips after.

On simplification, the $\widehat{U}$ is reduced to a 4×4 matrix such that

$$\widehat{U} = \frac{1}{2}e^{i\frac{\delta}{2}} \begin{pmatrix} e^{i\frac{\delta}{2}} - \Pi e^{-i\frac{\delta}{2}} & i\Pi(e^{i\frac{\delta}{2}} + \Pi e^{-i\frac{\delta}{2}}) \\ i\Pi(e^{i\frac{\delta}{2}} + \Pi e^{-i\frac{\delta}{2}}) & -(e^{i\frac{\delta}{2}} - \Pi e^{-i\frac{\delta}{2}}) \end{pmatrix}. \tag{12}$$

Therefore, our outputs in terms of our inputs can be evaluated as

$$\begin{pmatrix} E^c_{ij} \\ E^d_{ij} \end{pmatrix} \widehat{U} = \frac{1}{2}(e^{i\frac{\delta}{2}} \begin{pmatrix} e^{i\frac{\delta}{2}} - \Pi e^{-i\frac{\delta}{2}} & i\Pi(e^{i\frac{\delta}{2}} + \Pi e^{-i\frac{\delta}{2}}) \\ i\Pi(e^{i\frac{\delta}{2}} + \Pi e^{-i\frac{\delta}{2}}) & -(e^{i\frac{\delta}{2}} - \Pi e^{-i\frac{\delta}{2}}) \end{pmatrix} \begin{pmatrix} E^a_{ij} \\ E^b_{ij} \end{pmatrix}. \tag{13}$$

This simplifies to

$$\begin{pmatrix} E^c_{ij} \\ E^d_{ij} \end{pmatrix} = \frac{1}{2}(e^{i\frac{\delta}{2}} \begin{pmatrix} (e^{i\frac{\delta}{2}} - \Pi e^{-i\frac{\delta}{2}})E^a_{ij} + i\Pi(e^{i\frac{\delta}{2}} + \Pi e^{-i\frac{\delta}{2}})E^b_{ij} \\ i\Pi(e^{i\frac{\delta}{2}} + \Pi e^{-i\frac{\delta}{2}})E^a_{ij} - (e^{i\frac{\delta}{2}} - \Pi e^{-i\frac{\delta}{2}})E^b_{ij} \end{pmatrix}. \tag{14}$$

Now we substitute Π for an even mode(E_{00} or E_{11}) to be 1 and Π for an odd mode (E_{10} or E_{01})to be -1, to get the following result,

$$\begin{pmatrix} E^c_{ij} \\ E^d_{ij} \end{pmatrix} = \begin{cases} \frac{1}{2}e^{i\frac{\delta}{2}} \begin{pmatrix} (e^{i\frac{\delta}{2}} - e^{-i\frac{\delta}{2}})E^a_{ij} + i(e^{i\frac{\delta}{2}} + e^{-i\frac{\delta}{2}})E^b_{ij} \\ i(e^{i\frac{\delta}{2}} + e^{-i\frac{\delta}{2}})E^a_{ij} - (e^{i\frac{\delta}{2}} - e^{-i\frac{\delta}{2}})E^b_{ij} \end{pmatrix} & : \Pi = 1 \\ \frac{1}{2}e^{i\frac{\delta}{2}} \begin{pmatrix} (e^{i\frac{\delta}{2}} + e^{-i\frac{\delta}{2}})E^a_{ij} - i(e^{i\frac{\delta}{2}} - e^{-i\frac{\delta}{2}})E^b_{ij} \\ -i(e^{i\frac{\delta}{2}} - e^{-i\frac{\delta}{2}})E^a_{ij} - (e^{i\frac{\delta}{2}} + e^{-i\frac{\delta}{2}})E^b_{ij} \end{pmatrix} & : \Pi = -1 \end{cases}$$

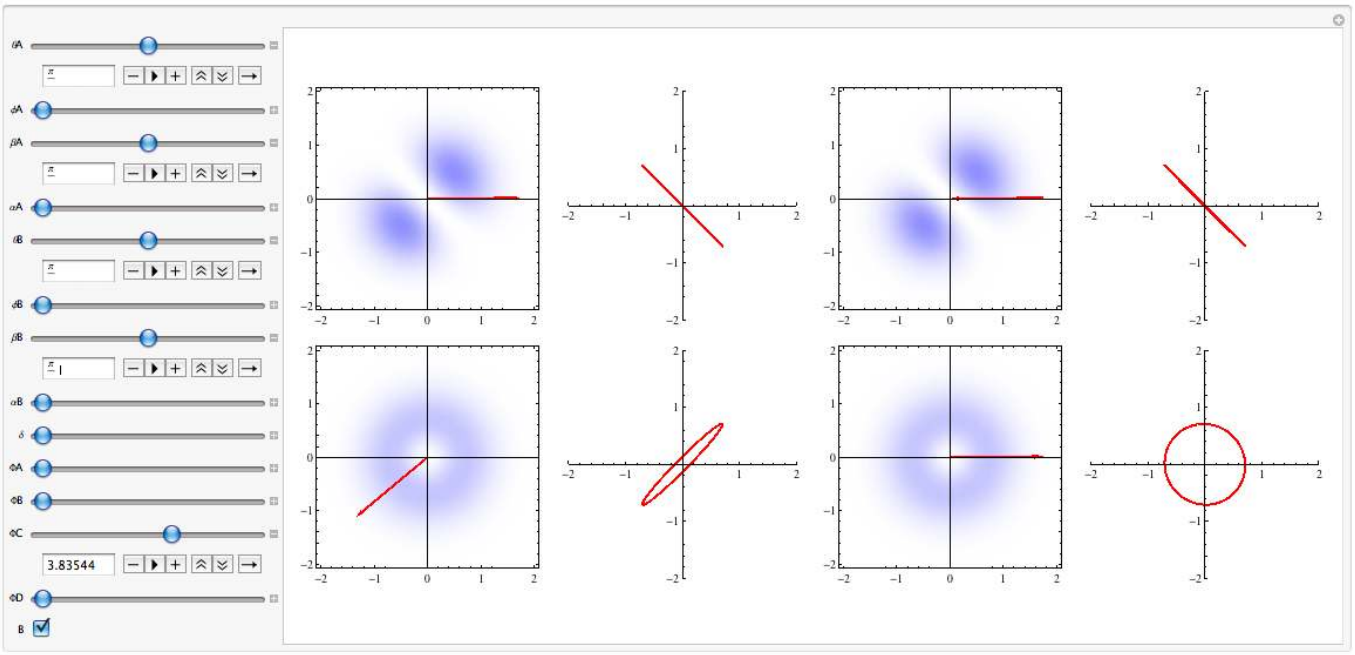

FIG. 13: The program simulation showing the various parameters that can be manipulated to show intensity and polarization plots. The inputs A and B in terms of density plots and polarization are described by the top two plots, while the bottom line represents the same for the outputs C and D.

On application of Euler's formula i.e. $e^{i\frac{\delta}{2}} = \cos\frac{\delta}{2} + i\sin\frac{\delta}{2}$, we have the following as functions of δ,

$$\begin{pmatrix} E^c_{ij} \\ E^d_{ij} \end{pmatrix} = \begin{cases} ie^{i\frac{\delta}{2}} \begin{pmatrix} \sin\frac{\delta}{2}E^a_{ij} + \cos\frac{\delta}{2}E^b_{ij} \\ \cos\frac{\delta}{2}E^a_{ij} - \sin\frac{\delta}{2}E^b_{ij} \end{pmatrix} & : \Pi = 1 \\ ie^{i\frac{\phi}{2}} \begin{pmatrix} -i(\cos\frac{\delta}{2}E^a_{ij} + \sin\frac{\delta}{2})E^b_{ij} \\ -i(\sin\frac{\delta}{2}E^a_{ij} - \cos\frac{\delta}{2}E^b_{ij}) \end{pmatrix} & : \Pi = -1 \end{cases}$$

This implies that when $\Pi = 1$, i.e. for even modes E_{00} and E_{11} and $\Pi = -1$, i.e. odd modes E_{10} and E_{01}, we are able to determine the outputs, so that Eq. 7 becomes,

$$\begin{pmatrix} e^c_{00} \\ e^d_{00} \\ e^c_{10} \\ e^d_{10} \\ e^c_{11} \\ e^d_{11} \\ e^c_{01} \\ e^d_{01} \end{pmatrix} = ie^{i\frac{\delta}{2}} \begin{pmatrix} \sin\frac{\delta}{2}e^a_{00} + \cos\frac{\delta}{2}e^b_{00} \\ \cos\frac{\delta}{2}e^a_{00} - \sin\frac{\delta}{2}e^b_{00} \\ -i(\cos\frac{\delta}{2}e^a_{10} + \sin\frac{\delta}{2}e^b_{10}) \\ -i(\sin\frac{\delta}{2}e^a_{10} - \cos\frac{\delta}{2}e^b_{10}) \\ \sin\frac{\delta}{2}e^a_{11} + \cos\frac{\delta}{2}e^b_{11} \\ \cos\frac{\delta}{2}e^a_{11} - \sin\frac{\delta}{2}e^b_{11} \\ -i(\cos\frac{\delta}{2}e^a_{01} + \sin\frac{\delta}{2}e^b_{01}) \\ -i(\sin\frac{\delta}{2}e^a_{01} - \cos\frac{\delta}{2}e^b_{01}) \end{pmatrix}, \tag{15}$$

Thus, it can be seen that the manipulation of the input states and the glass plate angle, changes the outputs coming out of the interferometer. These outputs are then programmed in *Mathematica* to visualize density plots for the various situations.

D. Visualization of Intensity distribution on *Mathematica*

To visualize the net field out port C we create density plots for the intensity distribution in *Mathematica* that is the electric field times its transpose conjugate written as

$$I = \vec{E}.\vec{E}^*. \tag{16}$$

The net electric field out port C is a given by

$$\vec{E}_c = e^c_{11}\hat{x} + e^c_{01}\hat{x} + e^c_{00}\hat{y} + e^c_{10}\hat{y} \tag{17}$$

which maybe rearranged in terms of the polarization degree of freedom to give

$$\vec{E}_c = (e^c_{11} + e^c_{01})\hat{x} + (e^c_{00} + e^c_{10})\hat{y}. \tag{18}$$

This can also be represented in column vector form as

$$\vec{E}_c = \begin{pmatrix} E_{cx} \\ E_{cy} \end{pmatrix} = \begin{pmatrix} e^c_{11} + e^c_{01} \\ e^c_{00} + e^c_{10} \end{pmatrix}. \tag{19}$$

Thus, to create a density plot for port C, we need the intensity i.e.

$$I_c = \vec{E}_c.\vec{E}^*_c = \begin{pmatrix} (e^c_{11} + e^c_{01}) & (e^c_{00} + e^c_{10}) \end{pmatrix} \cdot \begin{pmatrix} (e^c_{11} + e^c_{01})^* \\ (e^c_{00} + e^c_{10})^* \end{pmatrix}. \tag{20}$$

Similarly, the net field out port D was found and plotted in *Mathematica*. All the inputs and outputs can thus be seen in terms of density plots in Fig. 13.

E. Visualization of Polarization of the Output States

To be able to visualize the polarization of the output states, a *Mathematica* plot of elliptical polarization is created. Choosing elliptical polarization to represent these modes is important because elliptical polarization takes into account all other types of polarizations such as circular and linear. The modes had to be changed into cylindrical coordinates, so that they can be easily reduced to an equation that can determine the semimajor and semiminor axes and the orientation angle of a standard ellipse. This can be used to visualize the polarization of the output states.

Our fundamental Hermite Gaussian modes are thus now represented as,

$$HG_{01} = \sqrt{\frac{8}{\pi}}\rho \sin\Phi e^{-\rho^2} \tag{21}$$

and

$$HG_{10} = \sqrt{\frac{8}{\pi}}\rho \cos\Phi e^{-\rho^2} \tag{22}$$

where $\rho = \sqrt{x^2+y^2}$ and $x = \rho\cos\Phi$ and $y = \rho\sin\Phi$ where ρ and Φ are in cylindrical coordinates. Thus characterizing our output state of port C as a linear combination of the fundamental modes, we have,

$$\vec{E_c} = e^c_{11}\vec{E}_{11} + e^c_{01}\vec{E}_{01} + e^c_{00}\vec{E}_{00} + e^c_{10}\vec{E}_{10}. \tag{23}$$

Thus, using the cylindrical coordinate system, our electric field becomes,

$$\vec{E_c} = e^c_{11}HG_{10}\hat{x} + e^c_{01}HG_{01}\hat{x} + e^c_{00}HG_{01}\hat{y} + e^c_{10}HG_{10}\hat{y}. \tag{24}$$

On substitution, we find that the output becomes,

$$\vec{E_c} = \sqrt{\frac{8}{\pi}}\rho e^{-\rho^2}([e^c_{11}\cos\Phi + e^c_{01}\sin\Phi]\hat{x}$$

$$+[e^c_{00}\sin\Phi + e^c_{10}\cos\Phi]\hat{y}) \tag{25}$$

Each vector component of this expression may be represented as a complex number $A + iB$. Through this we have,

$$\vec{E_c} = \sqrt{\frac{8}{\pi}}\rho e^{-\rho^2}([A_x + iB_x]\hat{x} + [A_y + iB_y]\hat{y}) \tag{26}$$

The normalization of this equation represents a normalized Jones vector [9] that is commonly used in modern optics and is defined to be an arbitrary polarization vector, showing the x and y components of the field as

$$\vec{E}_{norm} = \frac{\vec{E}}{\vec{E}.\vec{E}^*} \tag{27}$$

This normalized vector is found to be

$$\vec{E}_{c_{norm}} = \frac{[A_x + iB_x]\hat{x} + [A_y + iB_y]\hat{y}]}{\sqrt{(A_x)^2 + (B_x)^2 + (A_y)^2 + (B_y)^2}}. \tag{28}$$

The normalized version tells us a lot about the dependence of polarization on factors of the electric field. It tells us that the cancellation of ρ shows us that there is no dependence on ρ for the output intensities. This independence of ρ implies that at any point on the same azimuthal cylindrical angle, we get the same polarization. This relationship reinforces the fact that these modes are cylindrically symmetric and only change with azimuthal angle.

Now, we reduce the standard form of a complex number $A + iB$ to $re^{i\phi}$ for both x and y components of our field. Thus, we now have,

$$\vec{E}_{c_{norm}} = \frac{\sqrt{(A_x)^2 + (B_x)^2}e^{i\tan^{-1}\frac{B_x}{A_x}}\hat{x}}{\sqrt{(A_x)^2 + (B_x)^2 + (A_y)^2 + (B_y)^2}}$$

$$+\frac{\sqrt{(A_y)^2 + (B_y)^2}e^{i\tan^{-1}\frac{B_y}{A_y}}\hat{y}}{\sqrt{(A_x)^2 + (B_x)^2 + (A_y)^2 + (B_y)^2}} \tag{29}$$

For the purposes of expressing the polarization state as a geometric ellipse, the electric field out port C is then expressed [10] in the form of,

$$\vec{E_c} = cos\Theta e^{i\Omega}\hat{x} + sin\Theta e^{i\Omega}\hat{y} \tag{30}$$

where $cos\Theta e^{i\Omega}$ is the coefficient of the net electric field in the $\hat{x}$ direction and $sin\Theta e^{i\Omega}$ is the coefficient of the net electric field in the $\hat{y}$ direction. Comparing Eq. 29 and Eq. 30 we have, the following result,

$$\Theta = \cos^{-1}\left[\frac{\sqrt{(A_x)^2 + (B_x)^2}}{\sqrt{(A_x)^2 + (B_x)^2 + (A_y)^2 + (B_y)^2}}\right]. \tag{31}$$

The value of Ω can also be found by comparing Eq. 29 and Eq. 30 so as to get two values of Ω, one in each direction, x and y. Thus,

$$\Omega_x = \tan^{-1}\frac{B_x}{A_x} \tag{32}$$

and the same for y,

$$\Omega_y = \tan^{-1}\frac{B_y}{A_y} \tag{33}$$

These values of Ω in each direction are then subtracted to get,

$$\Omega_{y-x} = \Omega_y - \Omega_x \tag{34}$$

Finally, we are ready to write out the semimajor and semiminor axes and the orientation angle of the ellipse

we want to plot. Thus, we have for the semimajor axis 'a' from [10] a relationship

$$a = |\vec{E_c}|\sqrt{\frac{1+\sqrt{1-\sin^2 2\Theta sin^2\Omega_{y-x}}}{2}}. \quad (35)$$

Similarly the semiminor axis of the ellipse [10] is given by

$$b = |\vec{E_c}|\sqrt{\frac{1-\sqrt{1-\sin^2 2\Theta sin^2\Omega_{y-x}}}{2}} \quad (36)$$

The orientation angle of the ellipse [10] that tells us at what angle the ellipse is oriented to the x-axis can also be determined through our calculations to be

$$\Gamma = \frac{1}{2}\tan^{-1}\left[\tan 2\Theta \cos\Omega_{y-x}\right] \quad (37)$$

The equation of an ellipse in *Mathematica* is parametrized using the semimajor and semiminor axes [11]. This will help us visualize the outputs C and D for their polarization as find in Fig. 13 where we see the polarization plots. The same was also performed for the inputs A and B, such the program is now able to give us the polarization and intensity distribution information as can be seen in Fig. 13 whenever arbitrary inputs are selected using the manipulate command in *Mathematica*.

III. PROCEDURE AND SIMULATION

This project was an expansion of the investigation of Hong-Ou-Mandel interference by manipulation of the photon spatial wave function by parity [2] & [3]. The basis of this model is thus the previous model that was worked on last summer and early this year. A large part of the basic calculation for this project was done by hand and then fed into *Mathematica* such that we are able to understand and gain intuition in the field, and the working of the interferometer.

A. Intensity Visualization

The idea behind the program was to visualize the outputs for such an interferometer in terms of density plots and polarization angles. The density plot command was used to visualize the intensity distribution of the spatial modes for both inputs and the outputs that can be described by the theory described previously.

The program [6] was created to visualize the electric field of the fundamental modes and the lobes. The next steps were to understand the theory behind the interferometer and be able to use matrix methods as shown in the theory to exploit the linear algebra and make the math manageable to compute the outputs. A module with all the computations for the output densities of ports C and D was created [11] using the input parameter of A and B. The parametrization of each input port comprises the angle θ and ϕ, β and α representing a unique mode on the Bloch Sphere having a unique polarization. The glass plate rotation is given by a change in δ. This can also be manipulated in the program simulation as shown in Fig. 13.

B. Polarization Visualization

To be able to visualize the polarization, we had to manipulate and reduce the output electric field for C and D outputs to a form that we can use to plot geometric ellipses. This comprised extracting relevant information as in Eq.35, Eq.36 and Eq.37 for the the semimajor axis a, semiminor axis b and the orientation angle Γ of the ellipse.

This information was fed into a parametric plot that is able to plot an ellipse to represent the polarization state at any cylindrical coordinate Φ. The cylindrical coordinate for the input and output intensity plots is a parameter to describe which point exactly on the density plot we would like to find the polarization. There is a manipulate knob on the program as can be seen in Fig. 13 where we can vary this parameter and visualize changes in polarization, if any. Thus, this accommodates for the fact that the polarization on each point of the density plot could change due to the interferometer elements and can't be simply predicted as the inputs that have the same polarization at every value for Φ. An arrow on the density plot can be used to describe the swinging azimuthal cylindrical coordinate Φ along the plot.

The potential to do both the single input and two-input case is created using the code to check port B. Thus we were able to extract information regarding intensity and polarization of the outputs through the simulation.

IV. RESULTS AND ANALYSIS

For the analysis of our theory, density plots on *Mathematica* were used and the results were drawn in analogy to our previous theoretical predictions and experiments, when polarization was not a variable parameter but always vertical. The aspects of the earlier model that we created have now been incorporated into this as well, such that our present simulation is powerful in giving us the output states of the photons and the polarization information.

To draw inferences into the case for Hong Ou Mandel interference, we use this model and study the outputs for certain inputs and see what we are able to get for the case of classical i.e. our model. The behavior of classical laser light and photons is exactly the same in this respect.

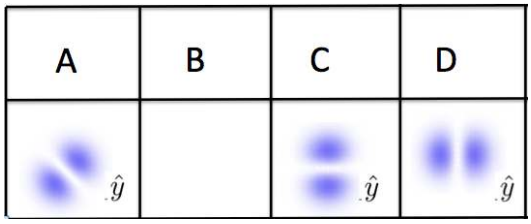

FIG. 14: Figure showing a sorter case for 1-D interferometer where the single input A is a 45° mode and the outputs C and D are the fundamental spatial modes. Thus the interferometer is 'sorting'.

A. 1-input case-$\delta = 0$

When we introduce one of the fundamental modes ($\theta = 0$ or $\theta = \pi$) into one of the inputs of the interferometer, i.e. even or odd Hermite Gaussian modes as in Fig. 2 and Fig. 3, we find that the output intensity distribution of the mode remains unchanged even though the polarization of the inputs is changed in the interferometer. As the glass plate angle δ is changed, the intensity of how much of the beam comes out of one port also changes flipping from complete constructive to complete destructive in C and D.

When we interfere any arbitrary mode, with vertical polarization into the 1-D parity interferometer, for the condition of the glass plate $\delta = 0$ we found that there will be sorting of modes into the even and odd compositions as in Fig 14. This result reinforces the fact that all arbitrary modes on the Bloch Sphere can be represented as superpositions of the fundamental even and odd modes. This was one of the earlier results as well. However, now we find that when an arbitrary polarization i.e. not vertical is introduced, the model acts no longer as a sorter. Another important result was that as we considered different cylindrical azimuthal angle, the polarization changes. This tells us that our device is capable of producing mixed or hybrid outputs while changing the intensity distribution of the outputs.

B. 1-input case-$\delta = \pi/2$

One of the most interesting conclusions we found as we were doing this experiment earlier, when the inputs were vertically polarized, was when we exploited the glass plate to see transformation of modes in our outputs, as we moved the glass plate in our one-dimensional interferometer. The most useful example for this was seen when we introduced two HG_{+45} or '+45' mode into the input and found two beams of the LG+ or donut mode coming out of the outputs. [3]

Now, we decided to investigate our inputs for $\delta = \pi/2$. When we introduce a vertically polarized fundamental mode into the interferometer, we find that there is no change in polarization or intensity.

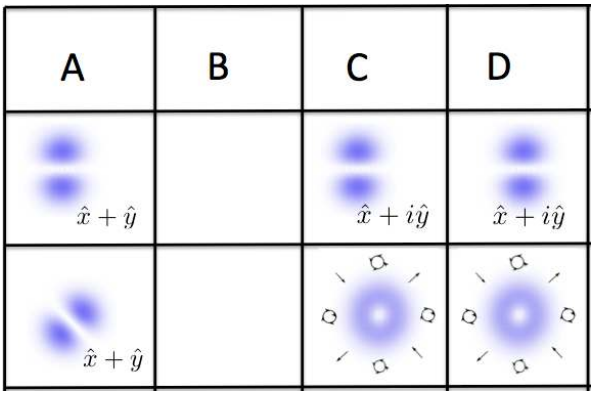

FIG. 15: A figure showing the outputs (C and D) when single input for $\delta = \pi/2$ is introduced in a 1-D interferometer

On the other hand, when the same fundamental mode is polarized linearly at an angle of $\pi/4$, we find that the outputs are the same in intensity but the polarization is now circular as in Fig. 15. The interference of photon spatial modes and polarization of these modes behave the same way. We are able to get an altered polarization keeping the intensity distribution the same. The polarization that we are testing in this case remains the same as the cylindrical azimuthal angle (Φ) is changed for the output mode.

The key idea that we learn from this is that by manipulating two degrees of freedom for a photon, we might be able to send two kinds of information without them interfering each other, thus leaving them intact after reaching the destination.

In the same scenario, i.e. one input, we introduce an HG_{+45} mode into the input and predict that the LG_{+} mode or donut is seen in terms of intensity distribution. When the polarization of this mode is set to 45°, we find that the outputs are circularly polarized for $\Phi = n\pi/2$ for n=0,1,2,3.. At $\Phi = n\pi/4$ for n=1,3,5,7, the output modes out of both ports are vertically polarized. In the intervals between these two, the modes are elliptically polarized. This modes has special significance in creating a mode that has a certain intensity distribution but arbitrary polarization at different Φ. To interpret this we use a linear polarizer and place it in line with a value of $\Phi = n\pi/2$ for n=0,1,2,3.. to observe an HG_{-45} mode which is an HG_{+45} rotated left 90° . On a deeper level, we might think of this situation as both degrees of freedom of a photon on being manipulated in an interferometer, interfering with each other and creating an interesting two-play of polarization and the spatial mode.

C. 2-input case-$\delta = \frac{\pi}{2}$

The two input case gives us indirect intuition for HOMI. We use similar inputs for A and B from earlier experiments and manipulate the polarization of the input beams.

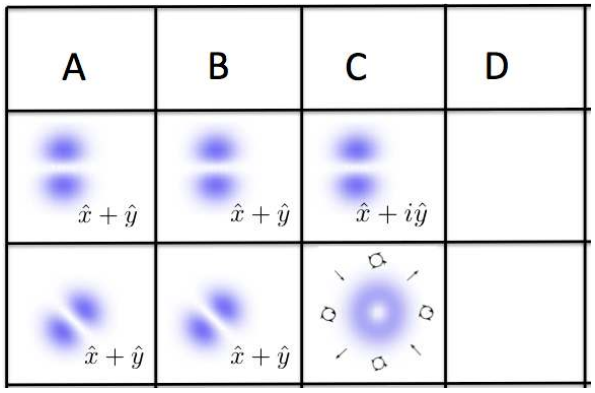

FIG. 16: Outputs when two inputs for $\delta = \pi/2$ introduced in 1-D interferometer

On introducing two identical even modes HG_{01} into the two inputs A and B of the interferometer with 45° polarization, we have a circularly polarized beam coming out of one port of the same intensity distribution as the inputs.

When we introduce two identical HG_{+45} modes as in Fig. 16 into the two inputs of the interferometer, we observe all the output coming out of one port. This is in analogy with the two photon interference case, as both photons would come out of only one port of the interferometer. When the polarization of the inputs is set to 45°, the output 'donuts' as predicted in the 1-input case have the interesting changing polarization(with Φ).

This kind of changing behavior in the two photon case could cause quantum entanglement of photons by entanglement of their states in two degrees of freedom. This kind of entanglement could be extremely useful for quantum computation.

V. CONCLUSIONS

The study of the manipulation of photon spatial wave function with respect to parity and polarization has applications to quantum computation because there lies a large potential in these interfering with one another and in remaining independent from each other.

When we look at the case when we manipulate the parity of the classical beam and observe the outputs when a fundamental even mode is introduced into the a single input of the interferometer, we find that outputs are also fundamental even modes as expected from earlier predictions, but on manipulating polarization such that the polarization is set to 45°, the output polarization is transformed into a circular polarization. Thus, the polarization behaves in a similar way to parity, transforming HG_{+45} modes to 'donuts'/circular polarization. At the same time, this behavior indicates that in this special case, these two degrees of freedom do not interfere with each other, i.e. the manipulation of polarization of the input does not affect the parity of the output and the manipulation of the polarization does not affect the parity. In this way, we might be able to send two kinds of information in a photon and being able to retrieve them at the receivers end without them interfering with each other.

On the other side, another special case was found when a classical HG_{+45} beam polarized at +45 is sent in through one port of an interferometer and the outputs observed are the LG_{+} modes that have varying polarization at different cylindrical azimuthal angle Φ. This leads us to predict another special case when both the parity and the polarization interfere with each other and may actually be entangled in a way that one correlates with the other.

When we extend a similar case to two inputs of the fundamental even mode but 45° polarization, there is a transformation of polarization into the circular and all the output out of one port. Similarly, we notice an HG_{+45} kind and 45° polarization, we are again able to create a situation when all the output comes out of one port and is of the donut form with varying polarization. This classical two-input case can be used to extend to our two photon HOMI case. As all the output comes out of one port, we can also predict both photons come out of the same port as in the case of HOMI. The output states of the photons are however not the same as we had in vertically polarized photons and vary with azimuthal angle as seen before.

Thus, this project has established that the degree of freedom of polarization of a classical beam or photon is not trivial for interactions with our interferometer and can be used for quantum information processing in sending two bits of information through manipulation of two degrees of freedom of the photon.

We understand that the polarization of a spatial mode can be manipulated in ways that can reinforce each other for correlation in quantum computing or be independent of each other and aid in transmitting two kinds of information without interference.

VI. ACKNOWLEDGEMENTS

I would like to thank my advisor, Dr. Cody Leary for his indispensable support, time and encouragement for the completion of this project. I also thank Dr. Lehman and the physics department at the College of Wooster for their support during the course of this project.

[1] C. K. Hong, Z.Y. Ou and L. Mandel., *Phys. Rev. Lett.* **59**, 2044-2046, (1987).

[2] D. Sundarraman, *The Magic $\hat{U}$ box; Bimodal Hong-Ou-*

Mandel interference in an interferometric optical system, Summer Research Report, (2012)
[3] T. Gilliss, *Manipulation of Transverse Photonic Degrees of Freedom Via Classical and Hong-Ou-Mandel Interference*, Senior Independent Study Thesis (2013)
[4] Abbondanzieri, E.A. et al., *Nature* **438**, 460-465, (2005).
[5] C. C. Leary, *Measurement and control of transverse photonic degrees of freedom via parity sorting and spin-orbit interaction*, Dissertation, U. Oregon, (2010)
[6] Dropbox/DeepikaJ.IS/VectorDensityPlotsmodesall.nb
[7] W. Shurcliff and S. Ballard, *Polarized Light*(D. Van Nostrand Company, Inc), **85**, (1964).
[8] R. Loudon, *The Quantum Theory of Light*(Oxford Science Publishing), **89**, (2000).
[9] James W. Lewis, Randall, Cora Einterz *Polarized Light in Optics and Spectroscopy*(Boston:Academic Press), **27**, (1990).
[10] Wikipedia, *http://en.wikipedia.org/wiki/Ellipticalpolarization*, Elliptical Polarization, (2012).
[11] Dropbox/DeepikaJ.IS/ABCDPolarizationIntensity.nb